

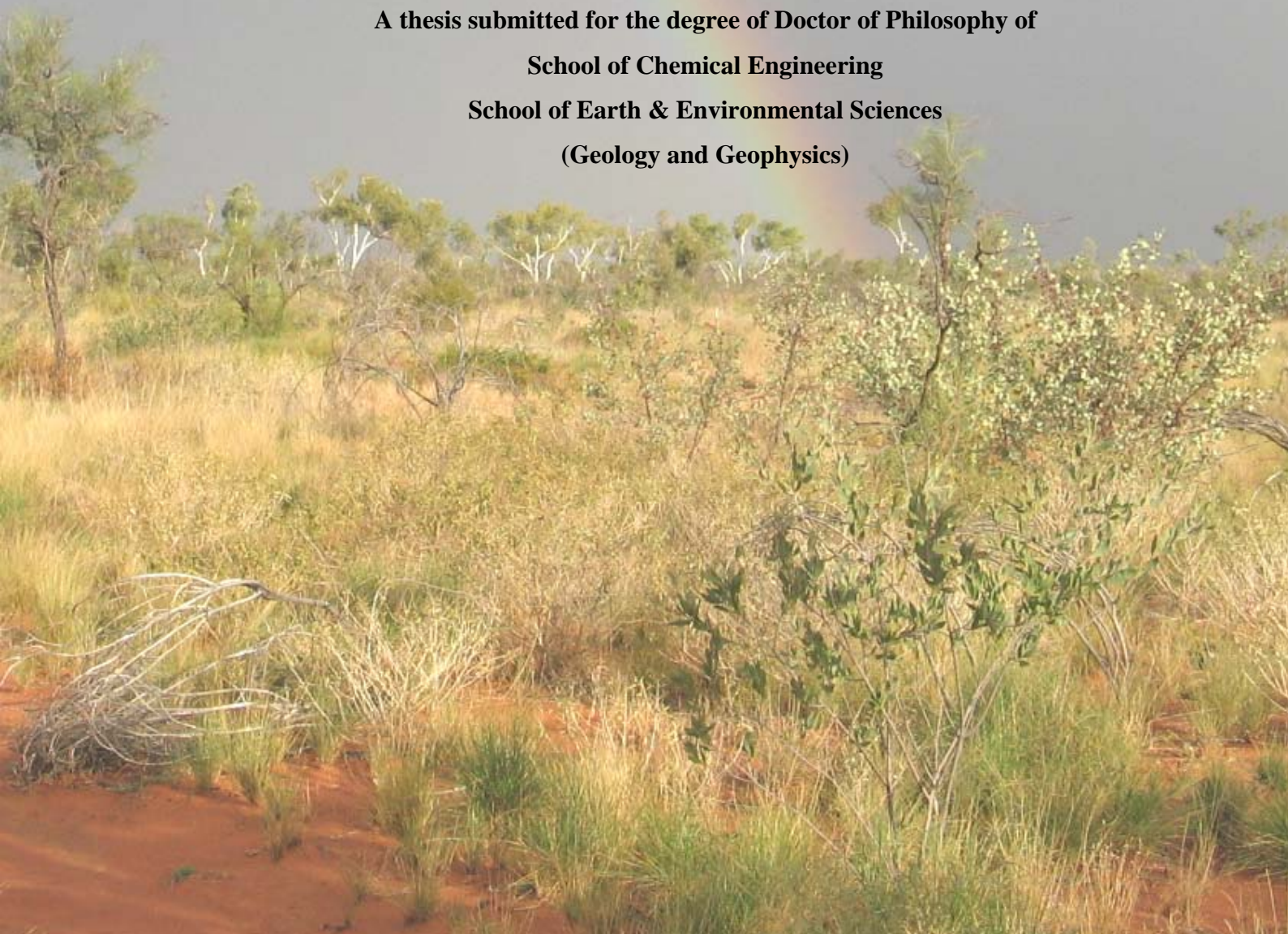


**Phyto-exploration in arid subtropical, arid mediterranean  
and tropical savanna environments: Biogeochemical  
mechanisms and implications for mineral exploration**

**Nathan Reid**

**June 2008**

**A thesis submitted for the degree of Doctor of Philosophy of  
School of Chemical Engineering  
School of Earth & Environmental Sciences  
(Geology and Geophysics)**



## **Declaration**

This work contains no material which has been accepted for the award of any other degree or diploma in any university or other tertiary institution and, to the best of my knowledge and belief, contains no material previously published or written by another person, except where due reference has been made in the text.

I give consent to this copy of my thesis when deposited in the University Library, being made available for loan and photocopying, subject to the provisions of the Copyright Act 1968.

The author acknowledges that copyright of published works contained within this thesis (as listed below) resides with the copyright holders of those works.

Reid, N., Hill, S. M. and Lewis, D. M., 2008. Spinifex biogeochemical expressions of buried gold mineralisation: the great mineral exploration penetrator of transported regolith. *Applied Geochemistry* 123, p76-84.

Signature:

Date:

## Acknowledgements

Special thanks to my supervisors Steve Hill and David Lewis who provided financial and moral support. Special thanks to other members of the CRC LEME Tanami Regolith Project team: Anna Petts, Lisa Worrall, Dirk Kirste, Brad Pillans and John Joseph. Thanks for assistance with sample preparation by Rodney King, Keryn Welk and David Kaczan. I thank CRC LEME, Newmont Asia Pacific, Tanami Gold NL and Australasia Gold for funding and support, with particular thanks to Steve Rogers, Karen Hulme, Robert Dart, Jessie Davey, Michael Neimanis, Damien Honner, Nigel Radford, Simon Bolster, James Anderson, Michael Green, Trevor Ireland and Brett Sando. Special thanks to Sally Moon, Sue Game, Helena Hink and Luisa Ruperto. Thanks for analyses performed by Genalysis Laboratories, Perth, and Acme Laboratories, Vancouver. And thanks to Ivan Holliday for the illustration of *Triodia pungens* below.



## Abstract

Vegetation sampling is an effective exploration technique in areas of transported cover where other techniques have been of limited success. Several plant species were sampled along transects across 9 known Au ore bodies; *Triodia pungens* was found give a Au, As,  $\pm$ Zn,  $\pm$ S,  $\pm$ Ce and  $\pm$ La signature which represented mineralisation through cover materials and *Eucalyptus brevifolia* was found to give a geobotanical and  $\pm$ Ca,  $\pm$ Mg, P, S and Zn signature of underlying geological structure. The Hyperion prospect was used as a 'blind' target as there was no background information available until after interpretation was carried out. Mineralisation was located at the contact between granite and dolerite, biogeochemical signatures from *E. brevifolia* and *Acacia bivenosa* showed areas of change in  $\pm$ Au, Ba, Ce,  $\pm$ Cu, La,  $\pm$ Mn, Nd, P, S, Sm, Y and Zn which corresponded to this contact. All species in the Pine Creek Orogen were able to present areas elevated in Au, As,  $\pm$ Zn,  $\pm$ S,  $\pm$ Mo and  $\pm$ Cu which provide future drilling targets. Biogeochemical sampling was able to determine the location of mineralisation at each site and identify underlying substrate changes, however, background knowledge relating to regolith, geology, hydrology and geophysics are important in aiding the interpretation of the elemental data as each component of the substrate influences the elements which a plant will uptake.

Mineral exploration in Australia has been driven by the search for large ore deposits close to the surface. This has led to the need to develop technologies for detecting mineral deposits under cover, which can be up to several hundred metres of transported sediments. The aim of this research was to test the feasibility of using vegetation biogeochemical sampling over known Au deposits within semi-arid and arid terrains. Biogeochemical sampling has the advantages of being cost effective, sustainable, environmentally friendly and relatively easy to perform.

Nine field sites were covered, 4 in the Tanami Region (Coyote, Larranganni, Hyperion and Titania), 4 in the Pine Creek Orogen (Johns Hill, Great Northern, Glencoe and McKinlay) and 1 in the Gawler Craton (Tunkillia). At each of these sites the dominant species were sampled and the elemental concentrations of the plant were analysed by Inductively Coupled Plasma Mass Spectrometry (ICP-MS) to test if they were able to detect buried mineralisation. In general, all species identified as being deep rooted (larger trees, paperbarks and spinifex) were able to detect mineralisation in each location within multi-element dispersion haloes centring over the projected ore body. Variations were dependant upon species differences and root structures, groundwater influences, and the potential for detrital contamination. In arid Australia, *Triodia spp.* were shown to be ideal for closely spaced tenement/prospect scale exploration, and *Heteropogon spp.* show similar trends for the humid tropics. *Eucalyptus/Corymbia spp.* are more suitable for widely spaced regional sampling exploration as they amalgamate a wider signal with strong groundwater influences.

It was found that all plant species were effective at expressing buried mineralisation in a multi-element suite (pathfinders: Au, As, S, Zn,  $\pm$ (Ce/La),  $\pm$ Mo and  $\pm$ Cu) through cover in these terrains provided care was taken with sampling and interpretation. Regolith materials, botanical properties and landforms are essential background knowledge for determining the effectiveness of biogeochemical sampling. Plants with deep root systems with little lateral spread are ideal for prospect/tenement mineral exploration programs, and plants with wide lateral spreads and large chemical uptake potentials are ideal for regional mineral exploration programs. This exploration strategy would be quick, sustainable and relatively cheap compared to other methods of exploration. This is not to say that biogeochemical sampling would be the only tool needed for further mineral exploration in Australia. This process would work best if used in conjunction with other sampling methods like geophysics and some soil sampling techniques.

## **Publications arising from this research**

Reid, N., Hill, S. M. and Lewis, D. M., 2005. Tanami Geobotany and Biogeochemistry: Towards its Characterisation, Role in Regolith Evolution and Implications for Mineral Exploration. *Regolith* **2005**, p256-259.

Worrall, L., Gibbons, L., Hill, S., Kirste, D., Petts, A., Pillans, B. and Reid, N., 2005. Fieldwork program completion report, 19-27 February 2005. CRC LEME Restricted Report 215R. Exploring through cover in the Tanami: A collaborative regolith research project.

Worrall, L., Hill, S., Kirste, D., Petts, A., Pillans, B. and Reid, N., 2005. Fieldwork program completion report, 4 - 14 October 2005. CRC LEME Restricted Report 225R. Exploring through cover in the Tanami: A collaborative regolith research project.

Reid, N., Hill, S. M. and Lewis, D. M., 2006. Geobotanical and Biogeochemical Associations of Snappy Gum (*Eucalyptus brevifolia*): Tanami Region, W.A. *Regolith* **2006**, p1-4.

Worrall, L., Petts, A. and Reid, N., 2006. Fieldwork program completion report 18 January - 4 February 2006. CRC LEME Restricted Report 247R. Exploring through cover in the Tanami: A collaborative regolith research project.

Worrall, L., Joseph, J., Kim, S., Kirste, D., Petts, A., Pillans, B. and Reid, N., 2006. Fieldwork program completion report 15 - 25 August 2006. CRC LEME Restricted Report 248R. Exploring through cover in the Tanami: A collaborative regolith research project.

Noble, R. R. P., Lintern, M. J., Reid, N. and Anand, R. R., 2007. Biogeochemistry and soil geochemistry of the North Miitel Prospect, Western Australia, CRC LEME Restricted Report 268R / E&M Report P2007/201.

Worrall, L., Joseph, J., Pillans, B., Kirste, D., Eggleton, T., Smith, M., Reid, N., Petts, A. and Hill, S. 2007. Targetting Callie-style gold mineralisation through the regolith in the Tanami Region. Annual Geoscience Exploration Seminar, Alice Springs, Northern Territory Geological Survey.

Reid, N. and Hill, S. M., 2007. Vegetation biogeochemistry and geobotany: Analytical report, CRC LEME Restricted Report 279R. Exploring through cover in the Tanami: A collaborative regolith research project.

Reid, N., Hill, S. M. and Lewis, D. M., 2008. Spinifex biogeochemical expressions of buried gold mineralisation: the great mineral exploration penetrator of transported regolith. *Applied Geochemistry* **123**, p76-84.

Reid, N., Hill, S. M. and Lewis, D. M., 2009. Biogeochemical expression of buried Au-mineralisation in semi-arid northern Australia: Penetration of transported cover at the Titania Gold Prospect, Tanami Desert Australia. *Geochemistry: Exploration, Environment, Analysis* **In Press**.

## Contents

1	Introduction.....	1
2	Biological and Geological Background and Linking Techniques .....	3
2.1	Geobotany .....	4
2.2	Biogeochemistry .....	5
2.3	Hyperaccumulation.....	8
2.4	Phyto-mining / remediation .....	9
2.5	Phyto-exploration.....	9
2.6	Botanical Information for Biogeochemistry Context .....	10
2.7	<i>Triodia spp.</i> detailed background .....	11
3	Methodology .....	13
3.1	Geobotanical methods.....	13
3.2	Biogeochemical methods.....	13
3.2.1	Sample collection.....	13
3.2.2	Sample preparation and analysis.....	14
3.2.3	Soil sampling .....	15
3.2.4	Quality assurance / quality control .....	15
3.2.5	Data analysis .....	16
3.3	Organ differentiation.....	17
3.4	Field site sampling summary .....	18
4	Tanami Region – Background .....	19
4.1	Introduction.....	19
4.2	Location and Geology.....	19
4.3	Landscape .....	21
4.4	Climate.....	22
4.5	Vegetation.....	23
4.6	Study sites .....	31
4.6.1	Coyote .....	31
4.6.2	Larranganni .....	35
4.6.3	Hyperion .....	35
4.6.4	Titania .....	36
5	Tanami Region – Species Results and Discussions.....	39
5.1	Geobotany and Biogeochemistry of the Coyote Deposit.....	39
5.1.1	Site specific methods .....	39
5.1.2	<i>Triodia pungens</i> (soft spinifex).....	41
5.1.3	<i>Eucalyptus brevifolia</i> (snappy gum).....	45
5.1.4	<i>Corymbia opaca</i> (desert bloodwood) .....	49
5.1.5	<i>Acacia coriacea ssp. sericophylla</i> (dogwood).....	53
5.1.6	<i>Eucalyptus pruinosa</i> (silver box).....	55
5.1.7	Species Differences.....	57
5.1.8	Elemental correlations .....	61
5.2	Biogeochemistry of the Larranganni Prospects .....	64
5.2.1	Site specific methods .....	64
5.2.2	<i>Eucalyptus brevifolia</i> (snappy gum).....	64
5.2.3	Elemental correlations .....	67
5.3	Biogeochemistry of the Hyperion Prospect .....	68
5.3.1	Site specific methods .....	68
5.3.2	<i>Eucalyptus brevifolia</i> (snappy gum).....	70
5.3.3	<i>Triodia pungens</i> (soft spinifex).....	72
5.3.4	<i>Acacia coriacea ssp. sericophylla</i> (dogwood).....	74
5.3.5	<i>Eucalyptus pruinosa</i> (silver box).....	75
5.3.6	<i>Acacia lysiphloia</i> (turpentine).....	78
5.3.7	Species Differences.....	80
5.3.8	Elemental correlations .....	83

5.4	Geobotany and Biogeochemistry of the Titania Prospect .....	88
5.4.1	Site specific methods .....	88
5.4.2	<i>Triodia pungens</i> (soft spinifex) .....	89
5.4.3	<i>Melaleuca lasiandra</i> (sandhill tea-tree).....	95
5.4.4	<i>Melaleuca glomerata</i> (inland paperbark) .....	99
5.4.5	<i>Acacia bivenosa</i> (two-nerved wattle) .....	102
5.4.6	<i>Acacia coriacea ssp. sericophylla</i> (dogwood).....	107
5.4.7	<i>Corymbia opaca</i> (desert bloodwood) .....	111
5.4.8	<i>Eucalyptus pachyphylla</i> (red-budded mallee) .....	114
5.4.9	<i>Grevillea striata</i> (beefwood) .....	117
5.4.10	<i>Hakea macrocarpa</i> (corkwood).....	120
5.4.11	Topsoil / Cryptogam samples .....	124
5.4.12	Species Differences .....	131
5.4.13	Elemental correlations .....	138
6	Tanami Region – Regional Summary and Discussion .....	145
6.1	Interpretation of spatial patterns .....	145
6.1.1	Coyote.....	145
6.1.2	Larranganni.....	146
6.1.3	Hyperion .....	147
6.1.4	Titania.....	147
6.2	Biogeochemical exploration model and recommended applications .....	148
6.3	Conclusions.....	149
7	Other Field Sites .....	151
7.1	Pine Creek Orogen – Background .....	151
7.1.1	Introduction.....	151
7.1.2	Previous work .....	151
7.1.3	Regional setting .....	152
7.1.4	Vegetation.....	153
7.1.5	Study sites .....	158
7.2	Pine Creek – Species Results and Discussions.....	159
7.2.1	Site specific methods .....	159
7.2.2	John’s Hill.....	160
7.2.3	Great Northern .....	164
7.2.4	Glencoe .....	171
7.2.5	McKinlay .....	176
7.2.6	Species Differences .....	182
7.2.7	Elemental Correlations .....	187
7.2.8	Pine Creek Orogen – Regional Summary and Discussion .....	191
7.3	Gawler Craton: Tunkillia Field Site – Background.....	194
7.3.1	Introduction.....	194
7.3.2	Previous work .....	195
7.3.3	Regional setting .....	195
7.3.4	Vegetation.....	196
7.4	Gawler Craton: Tunkillia Field Site –Results and Discussion .....	198
7.4.1	Elemental correlations .....	200
7.4.2	Discussion.....	204
8	Elemental Vectors and Processes .....	204
8.1	Elemental Variations .....	205
8.1.1	Between Species .....	205
8.1.2	Between Field Sites .....	205
8.2	Elemental Links .....	213
8.2.1	Depth.....	214
8.2.2	Mineralogy.....	214
8.2.3	Contamination.....	214

9	Summary design of phyto-exploration methodology .....	216
9.1	Regional Sampling Programs .....	216
9.2	Prospect and Tenement Scale Sampling Programs.....	217
9.3	Exploration Methodology .....	217
10	Conclusions.....	218
11	References.....	220
12	Appendix A: Raw data	Attached disk
13	Appendix B: Error analysis	Attached disk
14	Appendix C: Plant Dissection	Attached disk
15	Appendix D: Analytical Report of all results for the Tanami	Attached disk
16	Appendix E: Analytical Report of all results for Pine Creek	Attached disk
17	Appendix F: Published papers	Attached disk



## Table of Figures

Figure 1.1: Tanami, Pine Creek and Gawler Regions locations within Australia .....	1
Figure 2.1: Distribution of all spinifex species across Australia, adapted from AUSLIG 1990. .....	11
Figure 3.1: Samples being collected at the Coyote Prospect.....	14
Figure 3.2: Error analysis for the V14 standard reference material (Acme Laboratories and Dr. Colin Dunn 2006). .....	16
Figure 4.1: Location of all known Au deposits within the Tanami Region, taken from Huston <i>et al.</i> 2007. ....	21
Figure 4.2: <i>Acacia bivenosa</i> form, flowers and distribution, adapted from Moore 2005.....	23
Figure 4.3: <i>Acacia coriacea ssp. sericophylla</i> form, fruit and distribution, adapted from Moore 2005.....	24
Figure 4.4: <i>Acacia lysiphloia</i> form and distribution, adapted from Moore 2005 .....	24
Figure 4.5: <i>Corymbia opaca</i> form, galls and distribution, adapted from Moore 2005.....	25
Figure 4.6: <i>Eucalyptus brevifolia</i> and the related <i>Eucalyptus leucophloia</i> distribution, form and flowers, adapted from Moore 2005.....	25
Figure 4.7: <i>Eucalyptus pachyphylla</i> form, flowers and distribution, adapted from Moore 2005 .....	26
Figure 4.8: <i>Eucalyptus pruinosa</i> form, fruit and distribution, adapted from Moore 2005 .....	26
Figure 4.9: <i>Grevillea striata</i> form, leaves and distribution, adapted from Moore 2005 .....	27
Figure 4.10: <i>Hakea macrocarpa</i> form, flowers and distribution, adapted from Moore 2005 ..	27
Figure 4.11: <i>Melaleuca glomerata</i> form, flowers and distribution, adapted from Moore 2005 .....	28
Figure 4.12: <i>Melaleuca lasiandra</i> form, flowers and distribution, adapted from Moore 2005	28
Figure 4.13: Distribution of <i>Triodia pungens</i> adapted from Sharp & Simon 2002.....	29
Figure 4.14: Tussock form and ‘runner’ form of <i>Triodia pungens</i> . ....	30
Figure 4.15: Location of the 4 Tanami Prospects with respect to the nearest towns ( <a href="http://www.ga.gov.au/">http://www.ga.gov.au/</a> 2006).....	31
Figure 4.16: Interpreted geology across the Coyote and Larranganni prospects (Bagas <i>et al.</i> 2008).....	32
Figure 4.17: Interpreted geology of the Coyote prospect (Bagas <i>et al.</i> 2008).....	32
Figure 4.18: Geological section along 482300mE corresponding with the biogeochemical transect (Bagas <i>et al.</i> 2008) .....	33
Figure 4.19: Regolith-landform map across the Coyote prospect (Petts 2007a).....	34
Figure 4.20: Regolith cross section across the Coyote prospect, 42325mE, adapted from Tanami Gold drill logs.....	34
Figure 4.21: Geological cross sections of the Kookaburra and Sandpiper prospects (Bagas <i>et al.</i> 2007).....	35
Figure 4.22: Geological cross section north-south across the Hyperion prospect (Power 2004) .....	36
Figure 4.23: Geological cross section west-east across the Hyperion prospect corresponding with the biogeochemical transect (Power 2004).....	36
Figure 4.24: North-south geological cross section across the Titania prospect (Readford 1999) .....	37
Figure 4.25: Regolith-landform map across the Titania prospect (Petts 2007b).....	38
Figure 4.26: Regolith cross section across 603000mN, interpreted from Newmont drill logs	38
Figure 5.1: Vegetation distribution across the Coyote prospect.....	40
Figure 5.2: Species distribution map over the Coyote field site, with the study area within the black box. Ranges are interpreted from data points collected and remotely sensed data extrapolation. ....	41
Figure 5.3: Plots of S and Zn concentration in <i>Triodia pungens</i> overlying the orthophoto of the Coyote Prospect. The Au ore body, projected from 200 m depth, is within the area delineated by the black line. ....	42

Figure 5.4: Plots of As and Au concentration in <i>Triodia pungens</i> overlying the orthophoto of the Coyote Prospect. The Au ore body, projected from 200 m depth, is within the area delineated by the black line. ....	43
Figure 5.5: <i>Triodia pungens</i> elemental cross section across the Coyote transect.....	43
Figure 5.6: Arsenic comparison between soil and spinifex. ■ represents soil data with dotted line envelope. ▲ represents spinifex data with dashed line envelope. Mineralisation marked with a rectangle.....	44
Figure 5.7: Snappy gum locations along transect surrounding Coyote mineralisation. Fault zone is enclosed within the two white lines.....	46
Figure 5.8: Plots of As and S concentration for <i>Eucalyptus brevifolia</i> overlying the orthophoto of the Coyote Prospect. The Au ore body, projected from 200 m depth, is within the area delineated by the black line. ....	47
Figure 5.9: Plots of Zn (INAA) and Zn (ICP-MS) concentration for <i>Eucalyptus brevifolia</i> overlying the orthophoto of the Coyote Prospect. The Au ore body, projected from 200 m depth, is within the area delineated by the black line. ....	47
Figure 5.10: <i>Eucalyptus brevifolia</i> elemental cross sections across the Coyote transect.....	48
Figure 5.11: Uptake mechanism model, showing the root system of the snappy gum and its interaction with groundwater. ....	49
Figure 5.12: Plots of Al and As concentration for <i>Corymbia opaca</i> overlying the orthophoto of the Coyote Prospect. The Au ore body, projected from 200 m depth, is within the area delineated by the black line. ....	50
Figure 5.13: Plots of Zn (INAA) and Zn (ICP-MS) concentration for <i>Corymbia opaca</i> overlying the orthophoto of the Coyote Prospect. The Au ore body, projected from 200 m depth, is within the area delineated by the black line. ....	51
Figure 5.14: Plots of Au and Mo concentration for <i>Corymbia opaca</i> overlying the orthophoto of the Coyote Prospect. The Au ore body, projected from 200 m depth, is within the area delineated by the black line. ....	51
Figure 5.15: Plots of Al and Au concentration for <i>Acacia coriacea</i> overlying the orthophoto of the Coyote Prospect. The Au ore body, projected from 200 m depth, is within the area delineated by the black line. ....	53
Figure 5.16: Plots of Mn and Sr concentration for <i>Acacia coriacea</i> overlying the orthophoto of the Coyote Prospect. The Au ore body, projected from 200 m depth, is within the area delineated by the black line. ....	54
Figure 5.17: Plots of S and Sm concentration for <i>Acacia coriacea</i> overlying the orthophoto of the Coyote Prospect. The Au ore body, projected from 200 m depth, is within the area delineated by the black line. ....	54
Figure 5.18: Plots of As and Ce concentration for <i>Eucalyptus pruinosa</i> overlying the orthophoto of the Coyote Prospect. The Au ore body, projected from 200 m depth, is within the area delineated by the black line. ....	56
Figure 5.19: Plots of Ni and S concentration for <i>Eucalyptus pruinosa</i> overlying the orthophoto of the Coyote Prospect. The Au ore body, projected from 200 m depth, is within the area delineated by the black line. ....	56
Figure 5.20: Plots of K and Mg concentration for <i>Eucalyptus pruinosa</i> overlying the orthophoto of the Coyote Prospect. The Au ore body, projected from 200 m depth, is within the area delineated by the black line.....	57
Figure 5.21: Al results split by species at the Coyote Prospect.....	58
Figure 5.22: As results split by species at the Coyote Prospect. ....	58
Figure 5.23: S results split by species at the Coyote Prospect.....	59
Figure 5.24: Zn results split by species at the Coyote Prospect. ....	59
Figure 5.25: Co results split by species at the Coyote Prospect. ....	60
Figure 5.26: Cr results split by species at the Coyote Prospect.....	60
Figure 5.27: P results split by species at the Coyote Prospect.....	61
Figure 5.28: Ba INAA and Ba ICP visual correlation split by species at the Coyote Prospect. ....	62

Figure 5.29: Ca and Sr visual correlation split by species at the Coyote Prospect.....	63
Figure 5.30: Nd and Sm visual correlation split by species at the Coyote Prospect. ....	63
Figure 5.31: Cr and Fe visual correlation split by species at the Coyote Prospect.....	64
Figure 5.32: Plots of Au and As concentration for <i>Eucalyptus brevifolia</i> leaves overlying the orthophoto of the Larranganni Prospects.....	65
Figure 5.33: Plots of La and Ni concentration for <i>Eucalyptus brevifolia</i> leaves overlying the orthophoto of the Larranganni Prospects.....	65
Figure 5.34: Plots of Pb and U concentration for <i>Eucalyptus brevifolia</i> leaves overlying the orthophoto of the Larranganni Prospects.....	66
Figure 5.35: Elemental plots of <i>Eucalyptus brevifolia</i> across the Kookaburra-Sandpiper transect.....	66
Figure 5.36: Ba INAA and Ba ICP visual correlation at the Larranganni Prospects. ....	67
Figure 5.37: Sm and Nd visual correlation at the Larranganni Prospects. ....	68
Figure 5.38: Vegetation distribution across the Hyperion Prospect overlying the SPOT imagery. ....	69
Figure 5.39: Vegetation distribution across the Hyperion Prospect overlying regional magnetics imagery .....	69
Figure 5.40: <i>Eucalyptus brevifolia</i> elemental cross section across the Hyperion prospect.....	70
Figure 5.41: Plots of U (ICP-MS) concentration for <i>Eucalyptus brevifolia</i> overlying the SPOT of the Hyperion Prospect .....	71
Figure 5.42: Plots of As concentration for <i>Eucalyptus brevifolia</i> overlying the SPOT of the Hyperion Prospect .....	71
Figure 5.43: <i>Triodia pungens</i> elemental cross section across the Hyperion prospect.....	73
Figure 5.44: <i>Acacia coriacea</i> elemental cross section across the Hyperion prospect.....	74
Figure 5.45: REE plot of dogwood results normalised to chondrite at the Hyperion Prospect. ....	75
Figure 5.46: Plots of As concentration for <i>Eucalyptus pruinosa</i> overlying the SPOT of the Hyperion Prospect .....	76
Figure 5.47: Plots of Au concentration for <i>Eucalyptus pruinosa</i> overlying the SPOT of the Hyperion Prospect .....	76
Figure 5.48: Plots of Ce (ICP-MS) concentration for <i>Eucalyptus pruinosa</i> overlying the SPOT of the Hyperion Prospect .....	77
Figure 5.49: Plots of S concentration for <i>Eucalyptus pruinosa</i> overlying the SPOT of the Hyperion Prospect .....	77
Figure 5.50: <i>Acacia lysiphloia</i> elemental cross section across the Hyperion prospect .....	78
Figure 5.51: Plots of As concentration for <i>Acacia lysiphloia</i> overlying the SPOT of the Hyperion Prospect .....	79
Figure 5.52: Plots of S concentration for <i>Acacia lysiphloia</i> overlying the SPOT of the Hyperion Prospect .....	79
Figure 5.53: Al results split by species at the Hyperion Prospect. ....	80
Figure 5.54: Ca results split by species at the Hyperion Prospect.....	81
Figure 5.55: Ce results split by species at the Hyperion Prospect.....	81
Figure 5.56: Cr results split by species at the Hyperion Prospect. ....	82
Figure 5.57: P results split by species at the Hyperion Prospect.....	82
Figure 5.58: Al and Fe visual correlation split by species at the Hyperion Prospect. ....	84
Figure 5.59: As and Br visual correlation split by species at the Hyperion Prospect.....	84
Figure 5.60: Ba INAA and Ba ICP visual correlation split by species at the Hyperion Prospect.....	85
Figure 5.61: Ca and Sr visual correlation split by species at the Hyperion Prospect.....	85
Figure 5.62: Dy and Er visual correlation split by species at the Hyperion Prospect. ....	86
Figure 5.63: P and Nd visual correlation split by species at the Hyperion Prospect.....	86
Figure 5.64: S and Y visual correlation split by species at the Hyperion Prospect.....	87
Figure 5.65: Vegetation distribution across the Titania Prospect overlaying the orthophoto ..	88
Figure 5.66: Contoured vegetation map over the Titania field site. ....	89

Figure 5.67: Plots of As concentration for <i>Triodia pungens</i> overlying the orthophoto of the Titania Prospect. ....	90
Figure 5.68: Plots of Au concentration for <i>Triodia pungens</i> overlying the orthophoto of the Titania Prospect. ....	91
Figure 5.69: Plots of Zn concentration for <i>Triodia pungens</i> overlying the orthophoto of the Titania Prospect. ....	91
Figure 5.70: Plots of S concentration for <i>Triodia pungens</i> overlying the orthophoto of the Titania Prospect. ....	92
Figure 5.71: Plots of Al for <i>Triodia pungens</i> concentration overlying the orthophoto of the Titania Prospect. ....	92
Figure 5.72: Plots of U for <i>Triodia pungens</i> concentration overlying the orthophoto of the Titania Prospect. ....	93
Figure 5.73: Plots of Pb concentration for <i>Triodia pungens</i> overlying the orthophoto of the Titania Prospect. ....	93
Figure 5.74: Plots of As concentration for <i>Melaleuca lasiandra</i> overlying the orthophoto of the Titania Prospect. ....	95
Figure 5.75: Plots of Au concentration for <i>Melaleuca lasiandra</i> overlying the orthophoto of the Titania Prospect. ....	96
Figure 5.76: Plots of S concentration for <i>Melaleuca lasiandra</i> overlying the orthophoto of the Titania Prospect. ....	96
Figure 5.77: Plots of Zn concentration for <i>Melaleuca lasiandra</i> overlying the orthophoto of the Titania Prospect. ....	97
Figure 5.78: Plots of Al for <i>Melaleuca lasiandra</i> concentration overlying the orthophoto of the Titania Prospect. ....	97
Figure 5.79: Plots of U for <i>Melaleuca lasiandra</i> concentration overlying the orthophoto of the Titania Prospect. ....	98
Figure 5.80: Plots of As concentration for <i>Melaleuca glomerata</i> overlying the orthophoto of the Titania Prospect. ....	99
Figure 5.81: Plots of Au concentration for <i>Melaleuca glomerata</i> overlying the orthophoto of the Titania Prospect. ....	100
Figure 5.82: Plots of S concentration for <i>Melaleuca glomerata</i> overlying the orthophoto of the Titania Prospect. ....	100
Figure 5.83: Plots of Zn concentration for <i>Melaleuca glomerata</i> overlying the orthophoto of the Titania Prospect. ....	101
Figure 5.84: Plots of Ti concentration for <i>Melaleuca glomerata</i> overlying the orthophoto of the Titania Prospect. ....	101
Figure 5.85: Plots of U concentration for <i>Melaleuca glomerata</i> overlying the orthophoto of the Titania Prospect. ....	102
Figure 5.86: Plots of As concentration for <i>Acacia bivenosa</i> overlying the orthophoto of the Titania Prospect. ....	103
Figure 5.87: Plots of Au concentration for <i>Acacia bivenosa</i> overlying the orthophoto of the Titania Prospect. ....	103
Figure 5.88: Plots of S concentration for <i>Acacia bivenosa</i> overlying the orthophoto of the Titania Prospect. ....	104
Figure 5.89: Plots of Zn concentration for <i>Acacia bivenosa</i> overlying the orthophoto of the Titania Prospect. ....	104
Figure 5.90: Plots of Ca concentration for <i>Acacia bivenosa</i> overlying the orthophoto of the Titania Prospect. ....	105
Figure 5.91: Plots of Hf concentration for <i>Acacia bivenosa</i> overlying the orthophoto of the Titania Prospect. ....	105
Figure 5.92: Gypsum crystals precipitated onto the soil surface near the turkeys nest at the Titania prospect.....	107
Figure 5.93: Plots of As concentration for <i>Acacia coriacea</i> overlying the orthophoto of the Titania Prospect. ....	108

Figure 5.94: Plots of Au concentration for <i>Acacia coriacea</i> overlying the orthophoto of the Titania Prospect. ....	108
Figure 5.95: Plots of S concentration for <i>Acacia coriacea</i> overlying the orthophoto of the Titania Prospect. ....	109
Figure 5.96: Plots of Zn concentration for <i>Acacia coriacea</i> overlying the orthophoto of the Titania Prospect. ....	109
Figure 5.97: Plots of Al concentration for <i>Acacia coriacea</i> overlying the orthophoto of the Titania Prospect. ....	110
Figure 5.98: Plots of U concentration for <i>Acacia coriacea</i> overlying the orthophoto of the Titania Prospect. ....	110
Figure 5.99: Plots of As concentration for <i>Corymbia opaca</i> overlying the orthophoto of the Titania Prospect. ....	112
Figure 5.100: Plots of Au concentration for <i>Corymbia opaca</i> overlying the orthophoto of the Titania Prospect. ....	112
Figure 5.101: Plots of S concentration for <i>Corymbia opaca</i> overlying the orthophoto of the Titania Prospect. ....	113
Figure 5.102: Plots of Zn concentration for <i>Corymbia opaca</i> overlying the orthophoto of the Titania Prospect. ....	113
Figure 5.103: Plots of U concentration for <i>Corymbia opaca</i> overlying the orthophoto of the Titania Prospect. ....	114
Figure 5.104: Plots of Ce concentration for <i>Eucalyptus pachyphylla</i> overlying the orthophoto of the Titania Prospect. ....	115
Figure 5.105: Plots of Zn concentration for <i>Eucalyptus pachyphylla</i> overlying the orthophoto of the Titania Prospect. ....	115
Figure 5.106: Plots of S concentration for <i>Eucalyptus pachyphylla</i> overlying the orthophoto of the Titania Prospect. ....	116
Figure 5.107: Plots of Fe concentration for <i>Eucalyptus pachyphylla</i> overlying the orthophoto of the Titania Prospect. ....	116
Figure 5.108: Plots of As concentration for <i>Grevillea striata</i> overlying the orthophoto of the Titania Prospect. ....	117
Figure 5.109: Plots of Au concentration for <i>Grevillea striata</i> overlying the orthophoto of the Titania Prospect. ....	118
Figure 5.110: Plots of S concentration for <i>Grevillea striata</i> overlying the orthophoto of the Titania Prospect. ....	118
Figure 5.111: Plots of Zn concentration for <i>Grevillea striata</i> overlying the orthophoto of the Titania Prospect. ....	119
Figure 5.112: Plots of Fe concentration for <i>Grevillea striata</i> overlying the orthophoto of the Titania Prospect. ....	119
Figure 5.113: Plots of As concentration for <i>Hakea macrocarpa</i> overlying the orthophoto of the Titania Prospect. ....	121
Figure 5.114: Plots of Au concentration for <i>Hakea macrocarpa</i> overlying the orthophoto of the Titania Prospect. ....	121
Figure 5.115: Plots of Zn concentration for <i>Hakea macrocarpa</i> overlying the orthophoto of the Titania Prospect. ....	122
Figure 5.116: Plots of S concentration for <i>Hakea macrocarpa</i> overlying the orthophoto of the Titania Prospect. ....	122
Figure 5.117: Plots of Al concentration for <i>Hakea macrocarpa</i> overlying the orthophoto of the Titania Prospect. ....	123
Figure 5.118: Plots of As concentration for cryptogam samples overlying the orthophoto of the Titania Prospect. ....	124
Figure 5.119: Plots of Au concentration for cryptogam samples overlying the orthophoto of the Titania Prospect. ....	125
Figure 5.120: Plots of Zn concentration for cryptogam samples overlying the orthophoto of the Titania Prospect. ....	125

Figure 5.121: Plots of Ce concentration for cryptogam samples overlying the orthophoto of the Titania Prospect. ....	126
Figure 5.122: Plots of Ca concentration for cryptogam samples overlying the orthophoto of the Titania Prospect. ....	126
Figure 5.123: Plots of Cr concentration for cryptogam samples overlying the orthophoto of the Titania Prospect. ....	127
Figure 5.124: Plots of U concentration for cryptogam samples overlying the orthophoto of the Titania Prospect. ....	127
Figure 5.125: Plots of As concentration for cryptogam samples overlying the orthophoto of the Titania Prospect. ....	129
Figure 5.126: Plots of Au concentration for cryptogam samples overlying the orthophoto of the Titania Prospect. ....	129
Figure 5.127: Plots of Zn concentration for cryptogam samples overlying the orthophoto of the Titania Prospect. ....	130
Figure 5.128: Plots of Ce concentration for cryptogam samples overlying the orthophoto of the Titania Prospect. ....	130
Figure 5.129: Plots of S concentration for cryptogam samples overlying the orthophoto of the Titania Prospect. ....	131
Figure 5.130: As results split by species at the Titania Prospect.....	132
Figure 5.131: Au results split by species at the Titania Prospect. ....	132
Figure 5.132: Fe results split by species at the Titania Prospect. ....	133
Figure 5.133: S results split by species at the Titania Prospect.....	133
Figure 5.134: Zn results split by species at the Titania Prospect.....	134
Figure 5.135: Ca results split by species at the Titania Prospect.....	135
Figure 5.136: Co results split by species at the Titania Prospect. ....	135
Figure 5.137: Cr results split by species at the Titania Prospect. ....	136
Figure 5.138: Mg results split by species at the Titania Prospect.....	136
Figure 5.139: Mn results split by species at the Titania Prospect.....	137
Figure 5.140: Mo results split by species at the Titania Prospect.....	137
Figure 5.141: P results split by species at the Titania Prospect.....	138
Figure 5.142: Ca and S visual correlation split by species at the Titania Prospect. ....	138
Figure 5.143: Ca and Sr visual correlation split by species at the Titania Prospect. ....	139
Figure 5.144: Ce and La visual correlation split by species at the Titania Prospect. ....	139
Figure 5.145: Cr and Ni visual correlation split by species at the Titania Prospect.....	140
Figure 5.146: Cs and Fe visual correlation split by species at the Titania Prospect.....	140
Figure 5.147: Fe and Zr visual correlation split by species at the Titania Prospect. ....	141
Figure 5.148: K and Rb visual correlation split by species at the Titania Prospect. ....	141
Figure 5.149: Direct comparison between October 05 soil concentrations and August 06 soils. All concentrations are in ppm except for Ag, Au and Hg which are in ppb.....	142
Figure 5.150: Direct comparison between soil concentrations (Oct 05) and <i>Triodia pungens</i> concentrations. All concentrations are in ppm except for Ag, Au and Hg which are in ppb. ....	143
Figure 5.151: Direct comparison between soil concentrations (Oct 05) and <i>Melaleuca lasiandra</i> concentrations. All concentrations are in ppm except for Ag, Au and Hg which are in ppb. ....	143
Figure 5.152: Direct comparison between soil concentrations (Oct 05) and <i>Hakea macrocarpa</i> concentrations. All concentrations are in ppm except for Ag, Au and Hg which are in ppb. ....	144
Figure 5.153: Direct comparison between soil concentrations (Oct 05) and <i>Acacia bivenosa</i> concentrations. All concentrations are in ppm except for Ag, Au and Hg which are in ppb. ....	144
Figure 6.1: Stylised cross section of the Tanami showing materials beneath each field site and recommended sampling species.....	150

Figure 7.1 Leaves, fruit and distribution of <i>Brachychiton paradoxum</i> adapted from Brock 2001 .....	153
Figure 7.2: Form, flowers and distribution of <i>Calytrix achaeta</i> adapted from Brock 2001 ...	154
Figure 7.3: Form, leaves and distribution of <i>Cochlospermum fraseri</i> adapted from Brock 2001 .....	154
Figure 7.4: Form, leaves and distribution of <i>Corymbia polycarpa</i> adapted from Brock 2001 .....	155
Figure 7.5: Form, flowers and distribution of <i>Eucalyptus foelscheana</i> adapted from Brock 2001 .....	155
Figure 7.6: Form, leaves and distribution of <i>Eucalyptus miniata</i> adapted from Brock 2001.	156
Figure 7.7: Form, roots and distribution of <i>Heteropogon triticeus</i> adapted from Sharp & Simon 2002 .....	156
Figure 7.8: Form, flowers, roots and distribution of <i>Melaleuca viridiflora</i> adapted from Brock 2001 .....	157
Figure 7.9: Form, flowers and distribution of <i>Xanthostemon paradoxus</i> adapted from Brock 2001 .....	157
Figure 7.10: Location of the Pine Creek field sites with respect to major towns ( <a href="http://www.ga.gov.au/">http://www.ga.gov.au/</a> 2006).....	158
Figure 7.11: Spatial distribution of Au assay results for <i>Heteropogon triticeus</i> along the Johns Hill transect overlying the satellite imagery.....	160
Figure 7.12: <i>Heteropogon triticeus</i> elemental cross section across the Johns Hill transect....	161
Figure 7.13: Spatial distribution of Cu assay results for <i>Corymbia polycarpa</i> along the Johns Hill transect overlying the satellite imagery.....	162
Figure 7.14: <i>Corymbia polycarpa</i> elemental cross section across the Johns Hill transect.....	162
Figure 7.15: Spatial distribution of Cu assay results for <i>Melaleuca viridiflora</i> along the Johns Hill transect overlying the satellite imagery.....	163
Figure 7.16: <i>Melaleuca viridiflora</i> elemental cross section across the Johns Hill transect....	164
Figure 7.17: Spatial distribution of As assay results for <i>Heteropogon triticeus</i> along the Great Northern transect overlying the satellite imagery.....	165
Figure 7.18: Spatial distribution of Mo assay results for <i>Heteropogon triticeus</i> along the Great Northern transect overlying the satellite imagery.....	166
Figure 7.19: <i>Heteropogon triticeus</i> elemental cross section across the Great Northern transect .....	166
Figure 7.20: Spatial distribution of As assay results for <i>Eucalyptus foelscheana</i> along the Great Northern transect overlying the satellite imagery.....	168
Figure 7.21: Spatial distribution of Mo assay results for <i>Eucalyptus foelscheana</i> along the Great Northern transect overlying the satellite imagery.....	168
Figure 7.22: <i>Eucalyptus foelscheana</i> elemental cross section across the Great Northern transect.....	169
Figure 7.23: Spatial distribution of As assay results for <i>Melaleuca viridiflora</i> along the Great Northern transect overlying the satellite imagery.....	170
Figure 7.24: <i>Melaleuca viridiflora</i> elemental cross section across the Great Northern transect .....	170
Figure 7.25: Spatial distribution of Au and Cu assay results for <i>Heteropogon triticeus</i> along the Glencoe transect overlying the satellite imagery. Known mineralisation within the black lines.....	172
Figure 7.26: <i>Heteropogon triticeus</i> elemental cross section across the Glencoe transect.....	172
Figure 7.27: Spatial distribution of As and Au assay results for <i>Eucalyptus miniata</i> along the Glencoe transect overlying the satellite imagery. Known mineralisation within the black lines.....	173
Figure 7.28: <i>Eucalyptus miniata</i> (burnt) elemental cross section across the Glencoe transect .....	174

Figure 7.29: Spatial distribution of As and Au assay results for <i>Eucalyptus miniata</i> along the Glencoe transect overlying the satellite imagery. Known mineralisation within the black lines.....	175
Figure 7.30: <i>Eucalyptus miniata</i> (green) elemental cross section across the Glencoe transect .....	175
Figure 7.31: Spatial distribution of Au assay results for <i>Heteropogon triticeus</i> along the McKinlay transect overlying the satellite imagery. Known mineralisation is within the black line. ....	177
Figure 7.32: <i>Heteropogon triticeus</i> elemental cross section across the McKinlay transect ...	177
Figure 7.33: Spatial distribution of As assay results for <i>Corymbia polycarpa</i> along the McKinlay transect overlying the satellite imagery. Known mineralisation is within the black line. ....	178
Figure 7.34: <i>Corymbia polycarpa</i> elemental cross section across the McKinlay transect.....	179
Figure 7.35: Spatial distribution of As assay results for <i>Eucalyptus foelscheana</i> along the McKinlay transect overlying the satellite imagery. Known mineralisation is within the black line. ....	180
Figure 7.36: <i>Eucalyptus foelscheana</i> elemental cross section across the McKinlay transect	180
Figure 7.37: Spatial distribution of As assay results for <i>Eucalyptus miniata</i> along the McKinlay transect overlying the satellite imagery. Known mineralisation is within the black line. ....	181
Figure 7.38: <i>Eucalyptus miniata</i> elemental cross section across the McKinlay transect .....	182
Figure 7.39: As results split by species at the Pine Creek Prospects.....	182
Figure 7.40: Au results split by species at the Pine Creek Prospects. ....	183
Figure 7.41: Ce results split by species at the Pine Creek Prospects.....	183
Figure 7.42: Co results split by species at the Pine Creek Prospects.....	184
Figure 7.43: Cr results split by species at the Pine Creek Prospects. ....	184
Figure 7.44: Fe results split by species at the Pine Creek Prospects. ....	185
Figure 7.45: Mo results split by species at the Pine Creek Prospects.....	185
Figure 7.46: P results split by species at the Pine Creek Prospects. ....	186
Figure 7.47: Tl results split by species at the Pine Creek Prospects.....	186
Figure 7.48: Ce and La visual correlation split by species at the Pine Creek Prospects. ....	188
Figure 7.49: Cr and Ni visual correlation split by species at the Pine Creek Prospects. ....	188
Figure 7.50: Ce and Al visual correlation split by species at the Pine Creek Prospects.....	189
Figure 7.51: Fe and Zr visual correlation split by species at the Pine Creek Prospects. ....	189
Figure 7.52: K and P visual correlation split by species at the Pine Creek Prospects.....	190
Figure 7.53: S and P visual correlation split by species at the Pine Creek Prospects.....	190
Figure 7.54: U and Th visual correlation split by species at the Pine Creek Prospects.....	191
Figure 7.55: Location of the Tunkillia Prospect with respect to major towns ( <a href="http://www.ga.gov.au/">http://www.ga.gov.au/</a> 2006).....	194
Figure 7.56: Geological cross section across the Tunkillia mineralisation (Ferris & Wilson 2004).....	195
Figure 7.57: Distribution of <i>Triodia irritans</i> adapted from Sharp & Simon 2002. ....	197
Figure 7.58: Ring form and roots exposed of <i>Triodia irritans</i> at the Tunkillia Prospect.....	197
Figure 7.59: Spatial distribution of ashed As assay results for <i>Triodia irritans</i> along the Tunkillia transect. The white line represents the boundary of the Au resource with the ore body within this boundary. ....	198
Figure 7.60: Spatial distribution of ashed Au assay results for <i>Triodia irritans</i> along the Tunkillia transect. The white line represents the boundary of the Au resource with the ore body within this boundary. ....	199
Figure 7.61: <i>Triodia irritans</i> elemental cross section across the Tunkillia transect.....	199
Figure 7.62: Ca and Sr visual correlation at the Tunkillia Prospect. ....	200
Figure 7.63: Ce and La visual correlation at the Tunkillia Prospect. ....	201
Figure 7.64: Ce and Th (ashed) visual correlation at the Tunkillia Prospect. ....	201
Figure 7.65: Co and Cr visual correlation at the Tunkillia Prospect. ....	202



Figure 7.66: Cr and Cu visual correlation at the Tunkillia Prospect. ....	202
Figure 7.67: Cr and Ni visual correlation at the Tunkillia Prospect. ....	203
Figure 7.68: Fe and Zr visual correlation at the Tunkillia Prospect. ....	203
Figure 7.69: Th and Th (ashed) visual correlation at the Tunkillia Prospect. ....	204
Figure 8.1: As results split by site at the Tanami Prospects. ....	206
Figure 8.2: Au results split by site at the Tanami Prospects. ....	207
Figure 8.3: Ca results split by site at the Tanami Prospects. ....	207
Figure 8.4: Ce results split by site at the Tanami Prospects. ....	208
Figure 8.5: Cr results split by site at the Tanami Prospects. ....	208
Figure 8.6: Fe results split by site at the Tanami Prospects. ....	209
Figure 8.7: P results split by site at the Tanami Prospects. ....	209
Figure 8.8: S results split by site at the Tanami Prospects. ....	210
Figure 8.9: Au results split by site at the Pine Creek Prospects. ....	211
Figure 8.10: Cd results split by site at the Pine Creek Prospects. ....	211
Figure 8.11: Ce results split by site at the Pine Creek Prospects. ....	212
Figure 8.12: Cu results split by site at the Pine Creek Prospects. ....	212
Figure 8.13: Fe results split by site at the Pine Creek Prospects. ....	213
Figure 8.14: P results split by site at the Pine Creek Prospects. ....	213